

The Imaging Ultraviolet Spectrograph (IUVS) for the MAVEN Mission



William E. McClintock, Nicholas M. Schneider, Gregory M. Holsclaw, John T. Clark, Alan C. Hoskins, Ian Stewart, Franck Montmessin, Roger V. Yelle, Justin Deighan
Space Sci Rev, DOI 10.1007/s11214-014-0098-7

H. Nakagawa, 第40回火星勉強会, 論文紹介, 9, Dec., 2014.

紫外線高分解能分光によるリモート観測装置

1. Laboratory for Atmospheric and Space Physics (LASP) University of Coloradoで開発

2. Far-UVとMid-UVを広くカバー

3. 高分解能(これまでの周回機の中では最高)エッシェルモードでD/Hを観測

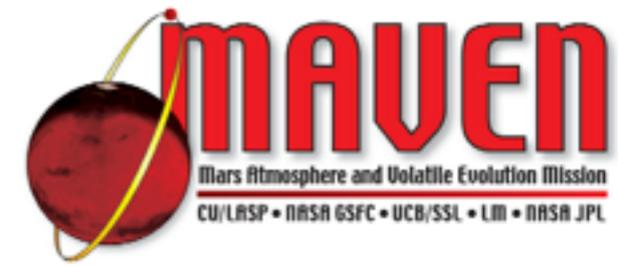
4. 装置独自にスキャン機構を持ちイメージング観測

(Articulated Payload Platform; APP and scan mirror)

5. 様々な大気光emission観測に特化

6. かなり優先的に観測sequencyが組まれている

Contents



1. Introduction (序論)

2. IUVS Science Objectives (何を観測する装置か)

3. Measurement Requirements (そのための要求精度)

4. Observing Strategy & Data Processing (観測戦略&データ処理)

5. Instrument Description (装置概要)

6. Measurement Performance (装置性能評価)

7. Conclusion (結論)

MAVEN



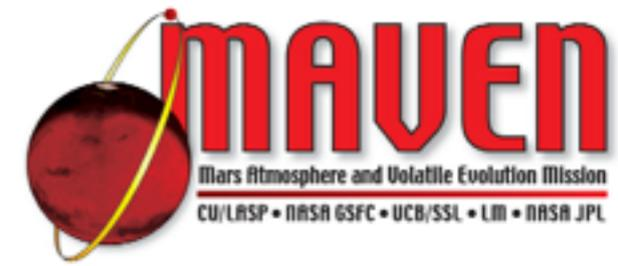
- **The goal of the mission is to obtain a comprehensive picture of the current state of the Mars upper atmosphere and ionosphere and the processes that control atmospheric escape.**
- **What is the current state of the upper atmosphere and ionosphere, and what processes control it?**
- **What are the rates of escape of atmospheric gases to space today and how do they relate to the underlying processes that control the upper atmosphere?**
- **What has been the total atmosphere loss to space through time?**

IUVS measures



- 熱圏中性大気(H,C,N,O,CO and N₂)とイオン(C⁺,CO₂⁺)の鉛直分布
- 超高層大気中のH,C,N,O,CO₂,O₃,ダストのカラム量
全球分布
- コロナ(H,D,and O)の鉛直分布
- 中間圏/熱圏のCO₂,O₃の鉛直分布
- 中間圏夜光

IUVS Objectives



高分解能で様々な分子・原子を精度よく観測

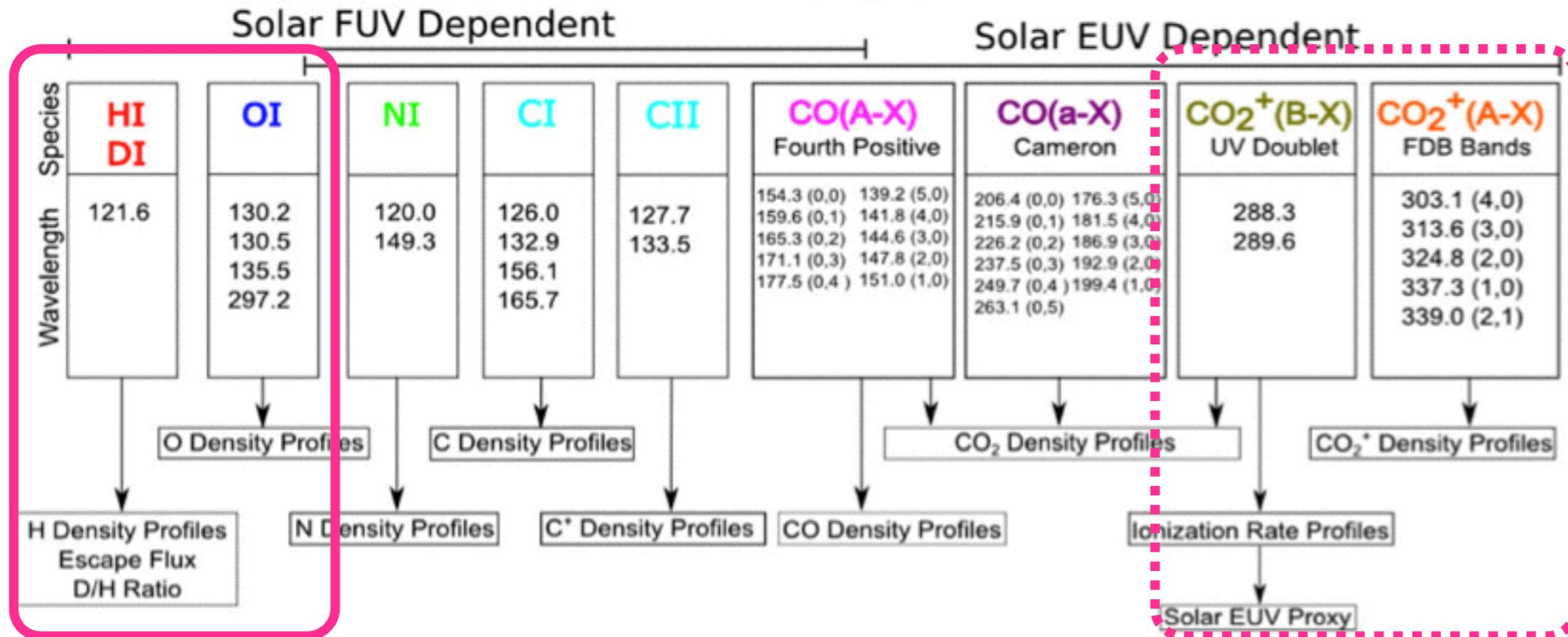
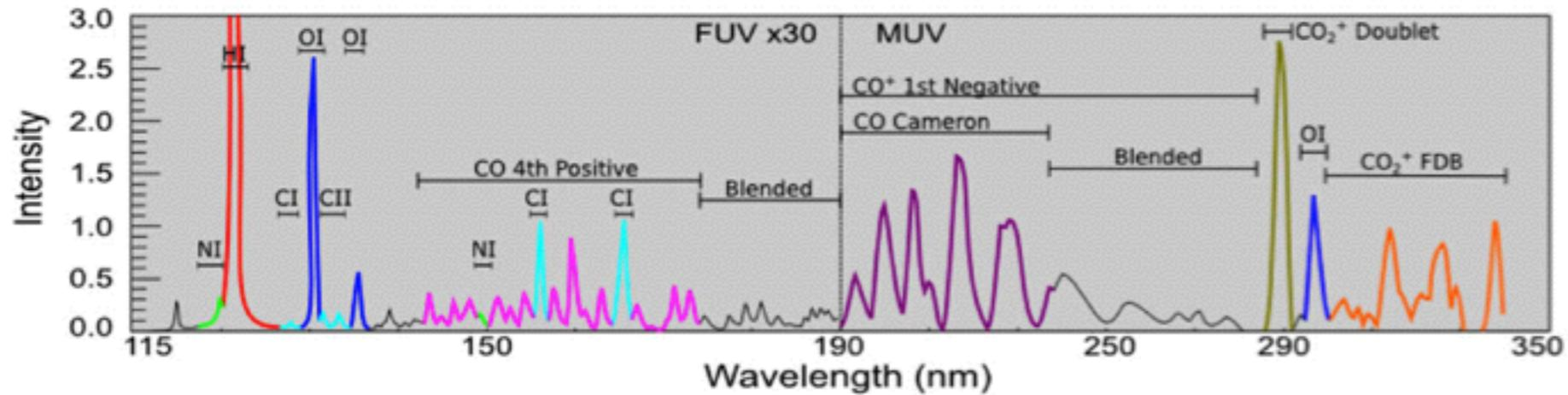
Table 1 IUVS Science Traceability Matrix

Measurement Requirements	Instrument and Spacecraft Requirements	Science Results
Global-Scale Composition and Structure	Imaging Ultra-Violet Spectroscopy	Derived Physical Quantities
	Observational Approach	Scientific Products
<p>Vertical profiles and column abundances of H, C, N, O, CO, N₂, and CO₂ from the homopause up to two scale heights (~ 1500 km for coronal H and O, ~24 km for CO₂) above the exobase with a vertical resolution of one scale height for each species and 25 % precision</p> <p>Vertical profiles and column abundances of C⁺ and CO₂⁺ from the ionospheric main peak up to the nominal ionopause with one CO₂⁺ scale height vertical resolution and 25 % precision</p> <p>D/H ratio above the homopause with sufficient precision (~30 %) to capture spatial/temporal variations (factor of 2) and compare with measured D/H in bulk atmosphere</p>	<p>115–330 nm wavelength range $\lambda/\Delta\lambda \sim 200$ nominal spectral resolution</p> <p>6 km vertical altitude resolution on the limb</p> <p>200 km horizontal at disk center from apoapsis</p> <p>$\lambda/\Delta\lambda \sim 12000$ nominal spectral resolution</p>	<p>Column densities and vertical profiles of H, C, N, O, CO, N₂, CO₂, C⁺ and CO₂⁺</p> <p>Scale heights, temperatures, and altitudes of the exobase and of the airglow layer peaks</p> <p>D/H ratio</p> <p>Spatial maps and vertical profiles of the atomic, molecular, and ion properties of the upper atmosphere and ionosphere, including the D/H ratio in the upper atmosphere</p> <p>Measurements of the neutral composition and structure of the corona</p>

様々な観測モードで中間圏から外圏までを幅広くカバー

超高分解能でD/Hを計測

IUVS spectrum



Other potentially observable features include the N₂ V-K band system, CO⁺(B-X), and the 131.7nm feature of CO(A-X). Spectral regions marked in grey are blended emissions and will not be used in pipeline processing.

Fig. 1 Predicted Mars FUV-MUV spectrum and flow down to retrieved quantities

各ラインで光るメカニズムが違う

Emission mechanism

メカニズムを知ることによって物理量に直せる

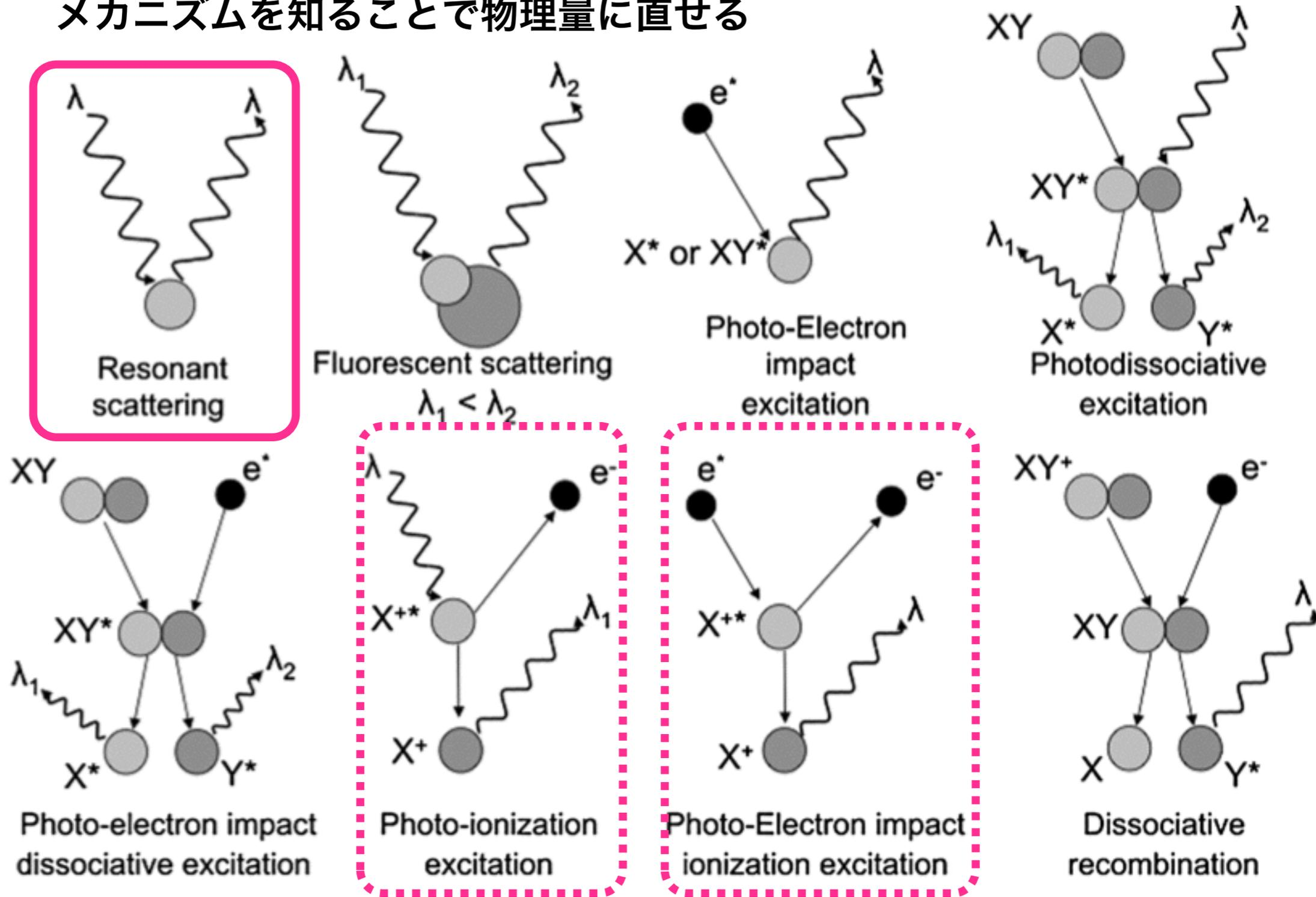


Fig. 2 Schemes of the different mechanisms leading to the dayglow. λ , λ_1 and λ_2 are the wavelength of the incident or emitted photons. X and Y are atoms, and e^- is an electron; X^+ or Y^+ is for a positive ion, and X^* , Y^* , XY^* , or X^{++} is an atom/molecule/ion in an excited state. From Leblanc et al. (2006)

Science Goals



- 超高層大気 in 100-225 km

- 原子・分子成分と温度の構造を明らかにする.

- 中間圏 in 30-100 km

MAVENで唯一中間圏まで観測

- ダイナミクスと光化学反応の様々な時空間変動を明らかにする.

- 火星コロナ above 200km

低高度軌道をとるため常にコロナ中から観測

- 中性大気の散逸量を計測する.

Instr. Requirements



Parameter	Requirement
Wavelength Coverage	
Composition and Structure	120–330 nm
Deuterium-to-Hydrogen	121.1–122.1 nm
Stellar Occultation	125–310 nm
Spectral Resolution	
Composition and Structure	0.6 nm (115–190 nm) and 1.2 nm (180–330 nm)
Deuterium-to-Hydrogen	0.009 nm ($R \sim 13,000$)
Stellar Occultation	2.5 nm (115–190 nm) and 5.0 nm (180–330 nm)
Spatial Coverage	
Altitude Range (Limb Scans)	90 km–220 km during periapsis passes
Spatial Resolution	
Thermosphere (Limb Scans)	12 km below 750 km altitude (CO_2 scale height)
Corona (Vertical Scans)	750 km above 750 km altitude (H and O)
Horizontal (Disk Maps)	170 km \times 170 km pixel footprint (3° aerocentric pixel)
Stellar Occultation	4 km vertical resolution
Field of View	
Limb Scans	0.176° (3 mrad) \times 11.25° (8 spatial elements)
Disk Maps	$1.4^\circ \times 11.25^\circ$ (10 spatial elements)
Deuterium-to-Hydrogen	0.057° (1 mrad) \times 1.7° (1 spatial element)
Stellar Occultation	$>0.6^\circ$ square
Field of Regard	
Limb Scans	24×10 Degrees
Disk Maps	60×10 Degrees
Radiometric Sensitivity	
Composition and Structure	$[\text{CO}]$, $[\text{CO}_2^+]$ 25 % precision, HCO , HCO_2^+ 15 % precision in 1 periapsis pass
Deuterium-to-Hydrogen	Measure D intensity to 30 % precision
Stellar Occultation	Top of Atmosphere SNR = 30 for $T_{\text{int}} = 2$ sec for the brightest stars

ノーマルモードでも十分高分解能
SPICAMと同程度(0.5nm)

そんなに厳しい数値ではないがスケールハイトを十分下回る。

非常に細かい構造をみたいわけではない

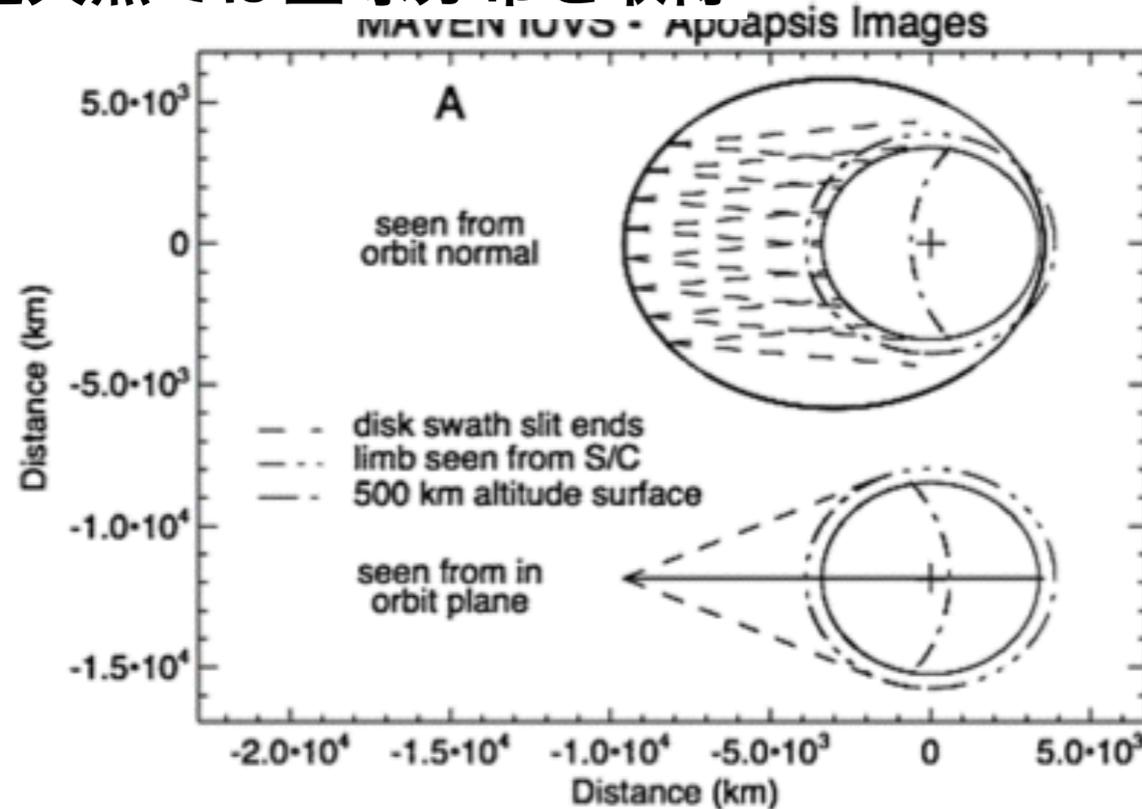
SPICAM(<10km for limb, 1km for occ.)

非常に高い精度を要求

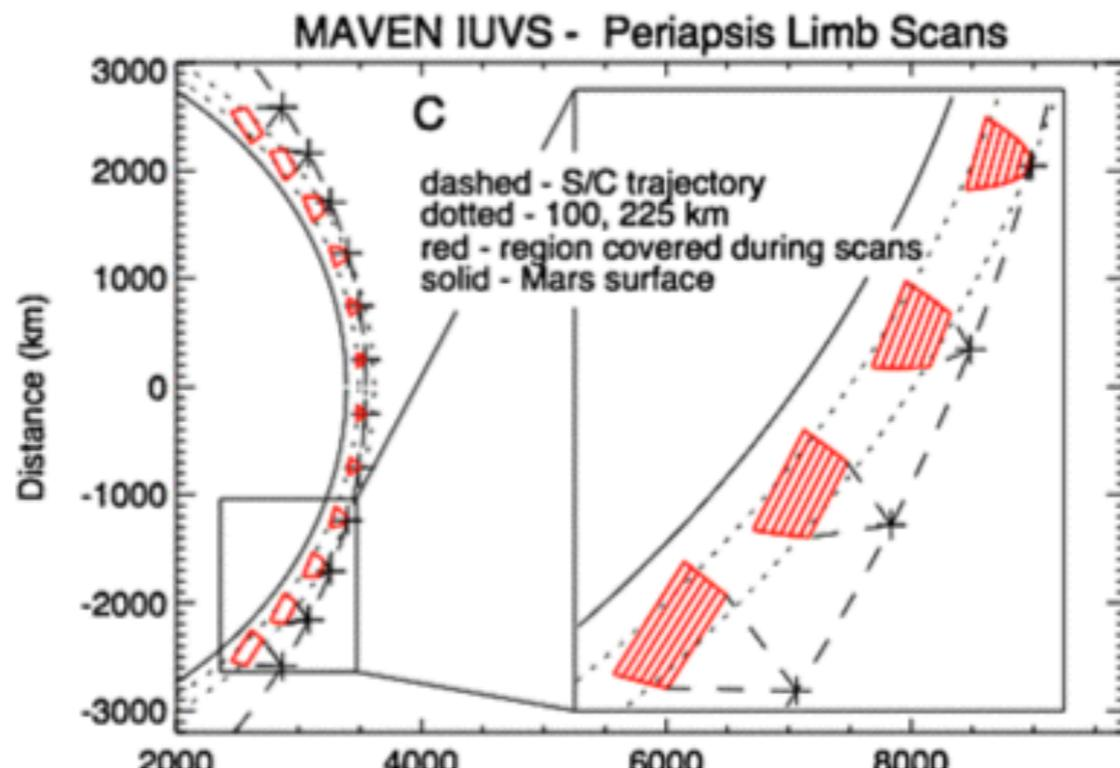
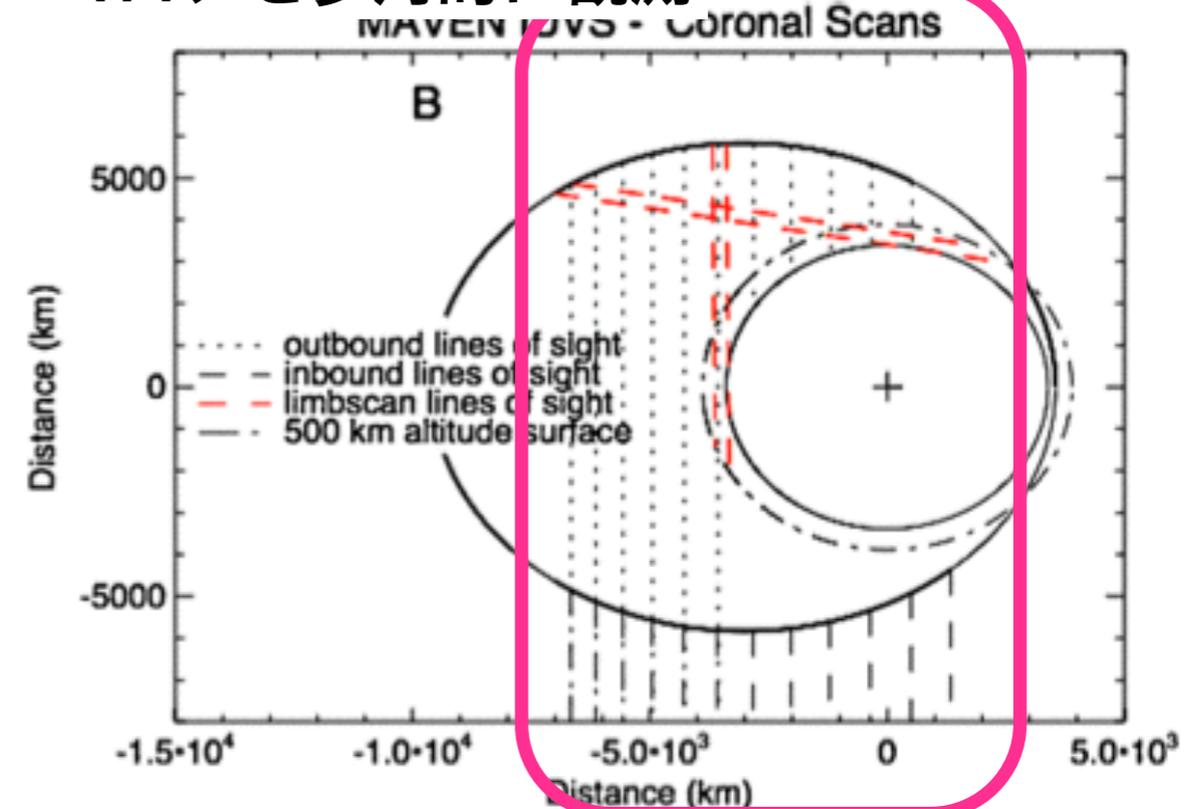
Observation Types



遠火点では全球分布を取得



コロナを多角的に観測

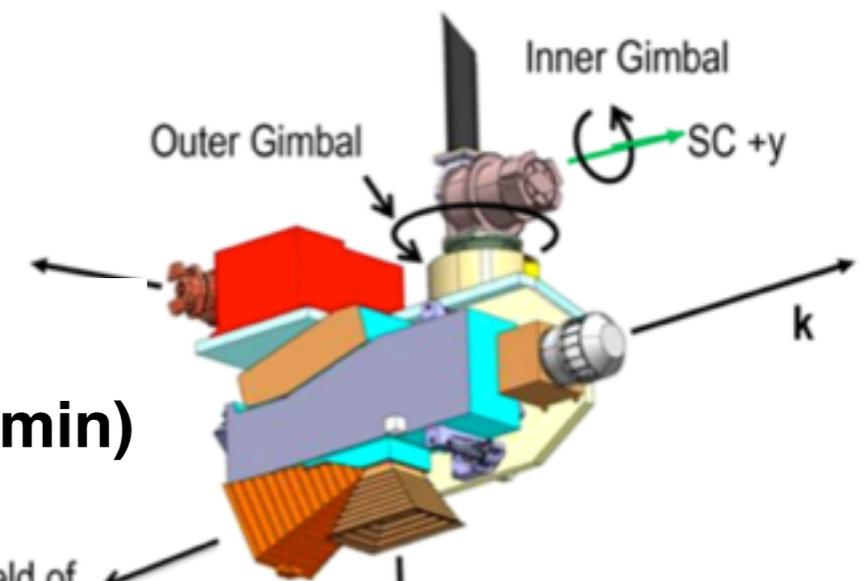


近火点では高い空間分解能で鉛直分布を取得

APP

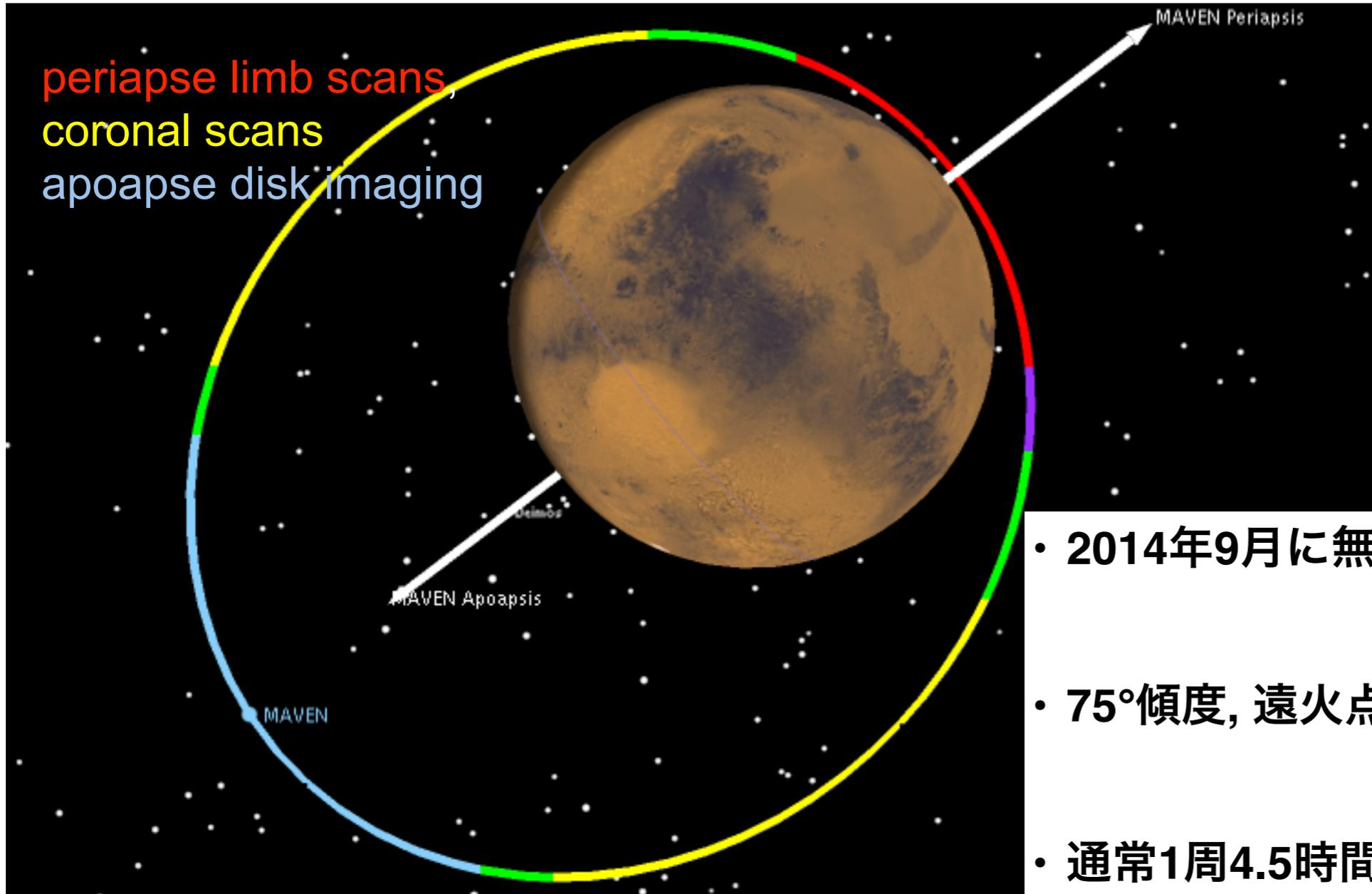
安定度

$\pm 0.3^\circ, \pm 0.25^\circ (4\text{min})$



独自のジンバルをもち2次元分布を取得
(MROでAPP自体は実証済み)

Orbit and Obs. Seq.



- 2014年9月に無事火星軌道

低い

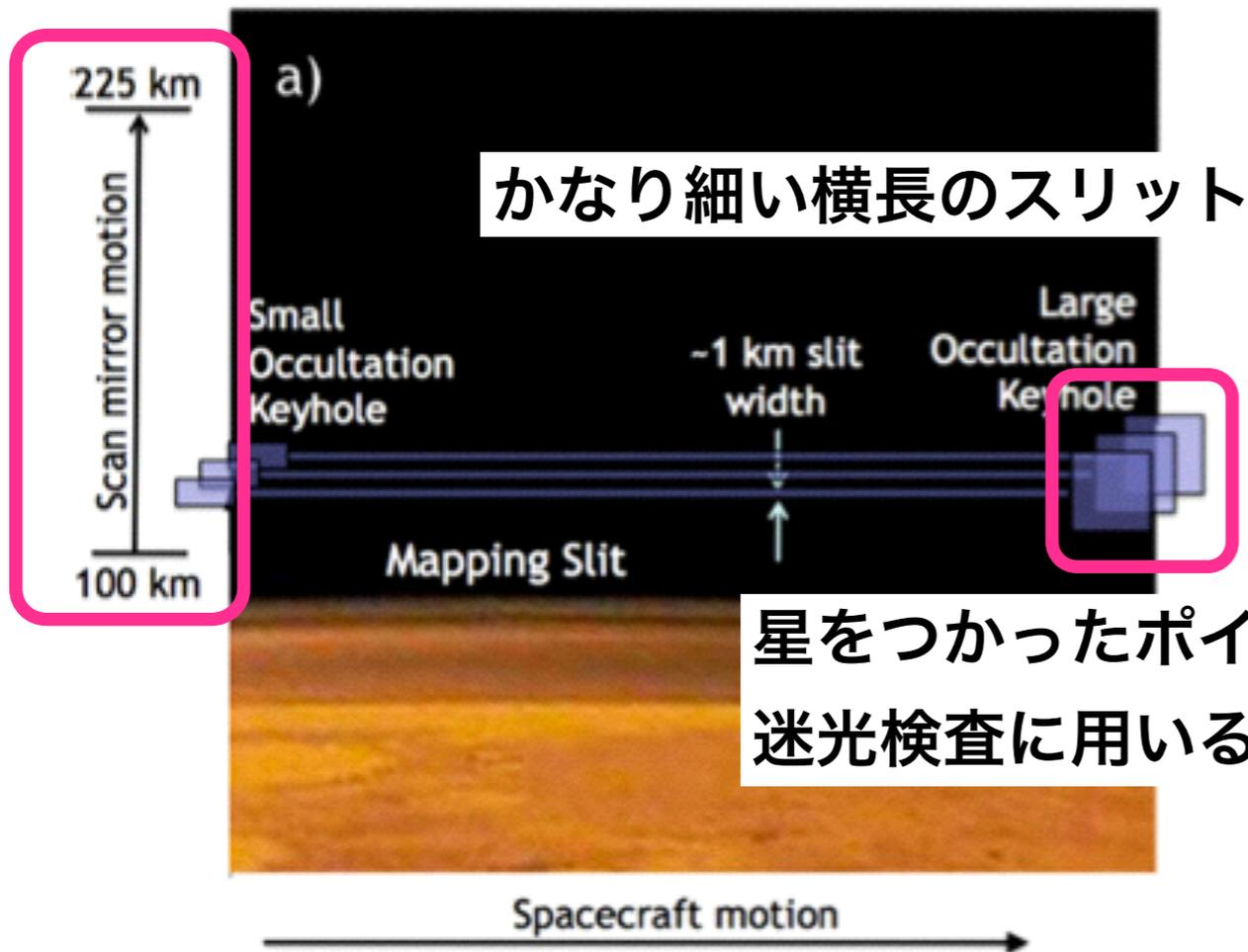
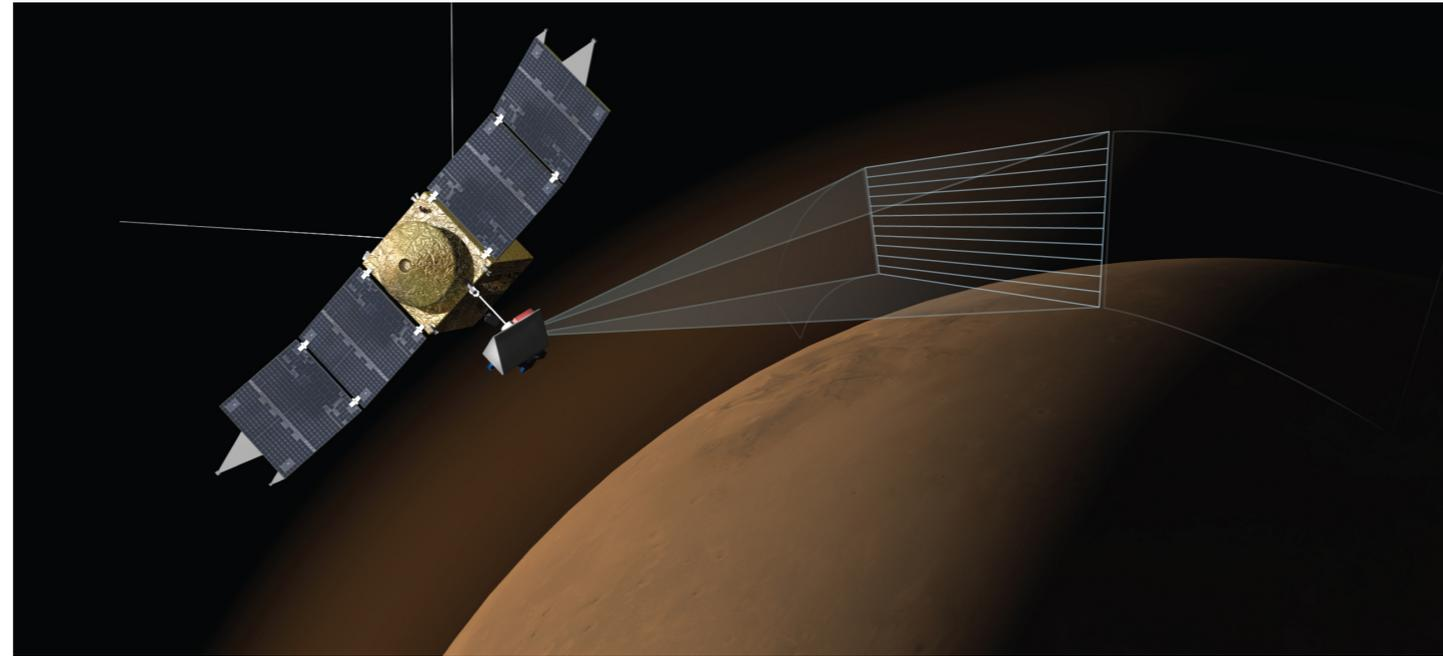
- 75°傾度, 遠火点6250km 近火点160km

- 通常1周4.5時間

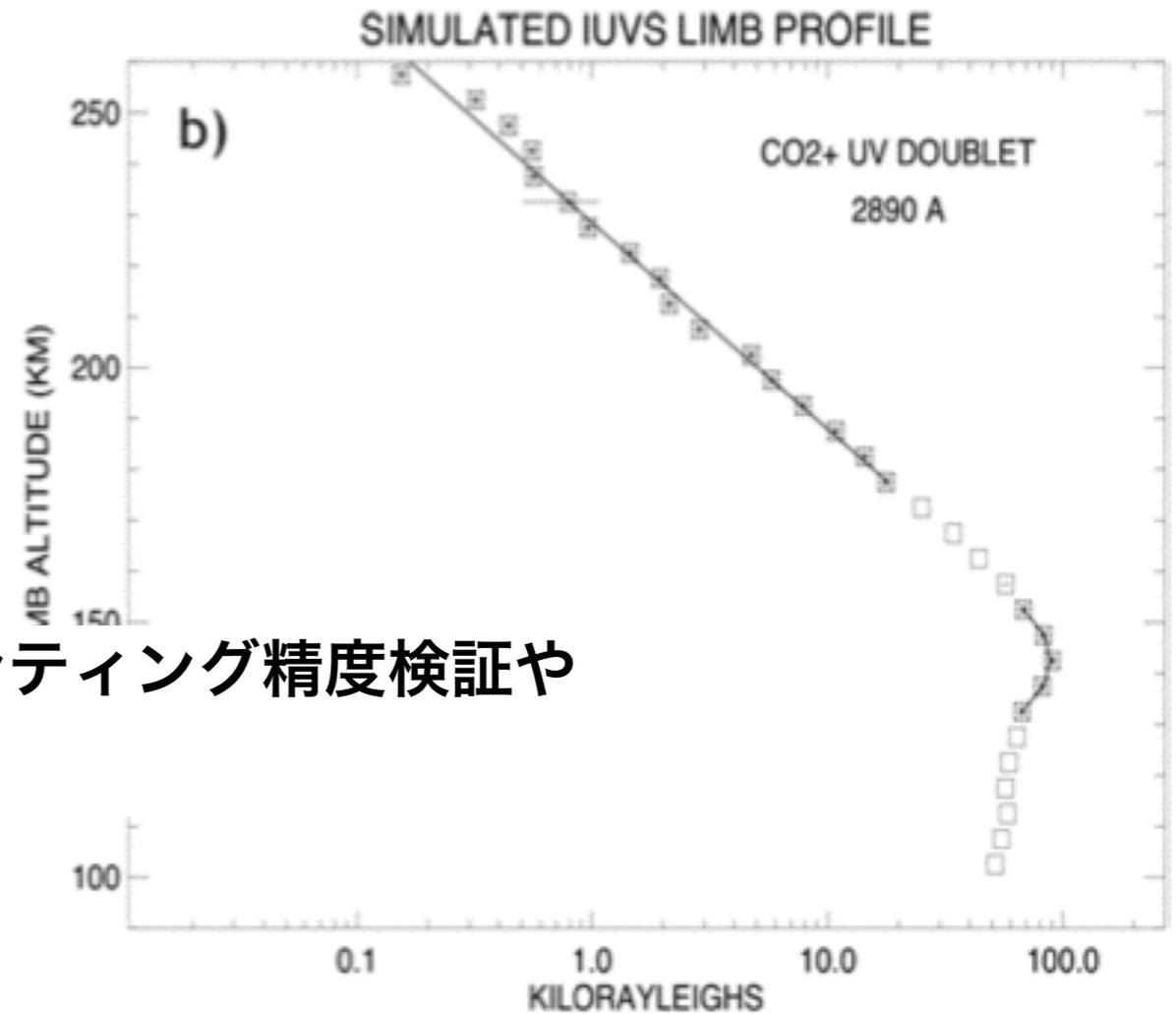
- ほぼすべての軌道上で観測

- 星掩蔽は1月から月1,2回?

Limb-Scan at Periapsis



星をつかったポインティング精度検証や
迷光検査に用いる。



Nadir-Scan at Apoaps

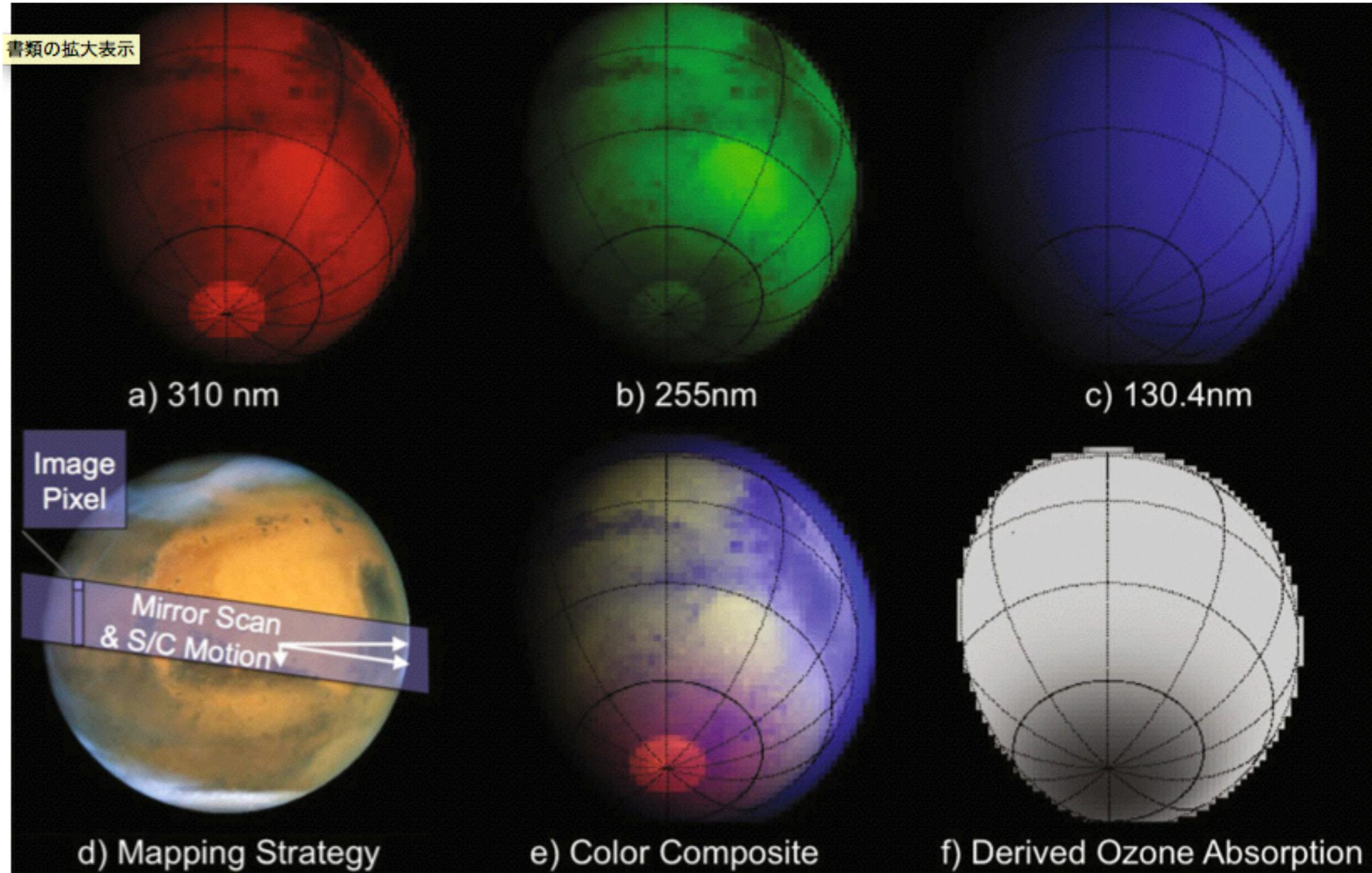


Fig. 6 IUVS disk maps. (d) IUVS uses a combination of spacecraft and scan mirror motion to construct global maps of the Mars atmosphere. Images at specific wavelengths are diagnostic of the surface and atmosphere. (a) Surface features are evident at 310 nm. (b) Attenuation from ozone absorption obscures the polar cap at 255 nm. (c) Atomic oxygen in the upper atmosphere can be seen at 130 nm. (e) A color composite using the images above combines all these phenomena. (f) A ratio of the 255 nm/310 nm images maps ozone

Data Processing



- データ転送レートに合わせて, 空間・波長方向にビンニングする(空間方向に8-20bin).
- DNs(data numbers)から暗電流, 宇宙線コンタミ, 迷光などの背景場を除去して, 最終的にRayleighs/nm(メガフォトン数)に変換.
- “L0: packets, L1A: raw data in DN, L1B: data calibrated in physical units & cleaned, L1C: spectrally and spatially processed data”
- まだ完全に迷光やコンタミを除去し切れていないのが現状

Instrument Design



Telescope

Aperture	13.3 × 20.0 mm
Focal length	100 mm
Field of Regard	
Limb	12.5° × 24°
Nadir	12.5° × 60°

要求空間分解能12kmで
決まる

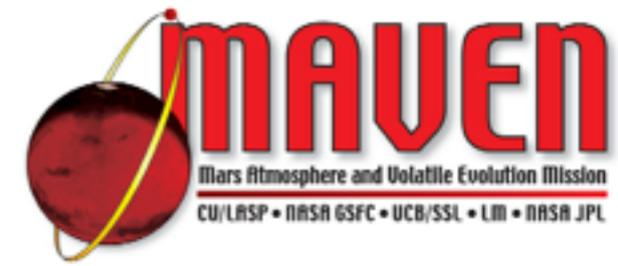
Ultraviolet Spectrograph—Normal Incidence Mode

Focal length	500 mm
Grating	
Ruling Density	286 groove/mm—blazed at 280 nm ⁽¹⁾
Projected Aperture	66.0 × 100.0 mm
Dispersion	
FUV detector	3.64 nm/mm (2nd order)
MUV detector	7.27 nm/mm (1st order)
Spectral resolution	
FUV detector	0.6 nm
MUV detector	1.2 nm
Wavelength range	
FUV detector	110–190 nm
MUV detector	180–340 nm
Field of View	
Atmosphere	0.06° × 11.3° (0.1 × 19.8 mm slit)
Occultation 1	0.29° × 0.4° (0.5 × 0.7 mm aperture)
Occultation 2	0.69° × 0.9° (1.2 × 1.6 mm aperture)

エッセル分散に最適化

(1) The grating vendor specification = 276 grooves/mm. The as-delivered = 286 grooves/mm

Instrument Design2



Ultraviolet Spectrograph—Echelle Mode

Focal length	500 mm
Grating	
Ruling Density	44.41 groove/mm—blazed at 69.85°
Projected Aperture	44.6 × 100.0 mm
Cross Disperser	MgF ₂ prism—apex angle = 7.5°
Echelle Dispersion	0.031 nm/mm (346th order)
Spectral resolution	14,500
Wavelength range	116–131 nm (362nd order–321st order)
Field of view	0.06° × 1.7° (0.1 × 3.0 mm slit)

Instrument

Mass		日本では考えられない重量・電力 c.f. SPICAM/MEX=9.0kg, 13W
IUVS	22.1 kg	
DPU+Harness	4.7 kg	
Average power		
IUVS+RSDPU	28.4 W	
Dimensions		
IUVS	61.7 × 54.1 × 23.1 cm ³	
RSDPU	25.0 × 32.0 × 9.9 cm ³	

- 分光器や検出器など、構成要素自体は新規要素で開発されたものではなく既存測器をベースに確実に達成. 但しHSTで搭載されていた高分解能分光器などをもとにしているため, これまで火星周回機ではなかった高分解能を達成.

Instrument



ビームスプリッタで
MUVとFUVを分離

高分解能エッシェルと
通常グレーティングを交換
(通常稼働部は作りたくない)

校正用ランプ

Fig. 9 IUVS optical schematic in the normal-incidence grating

mirror, N—normal incidence grating, M2—spectrograph camera mirror. SPT—beam

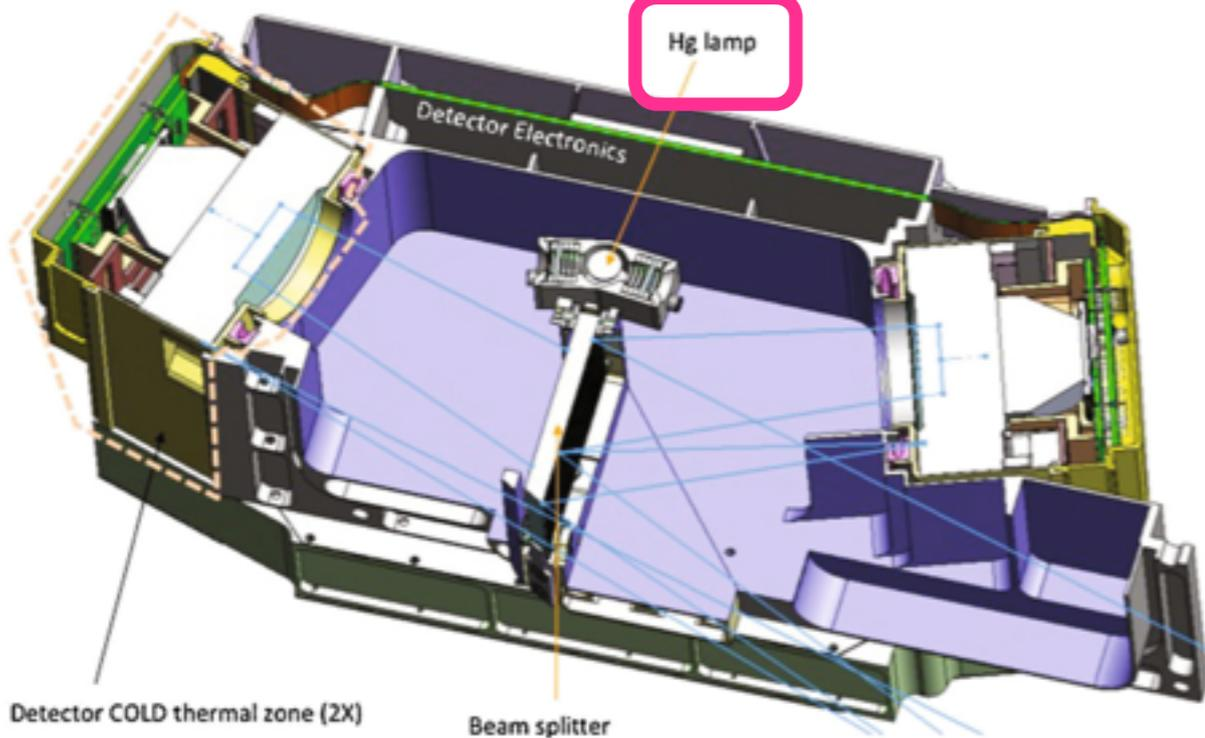
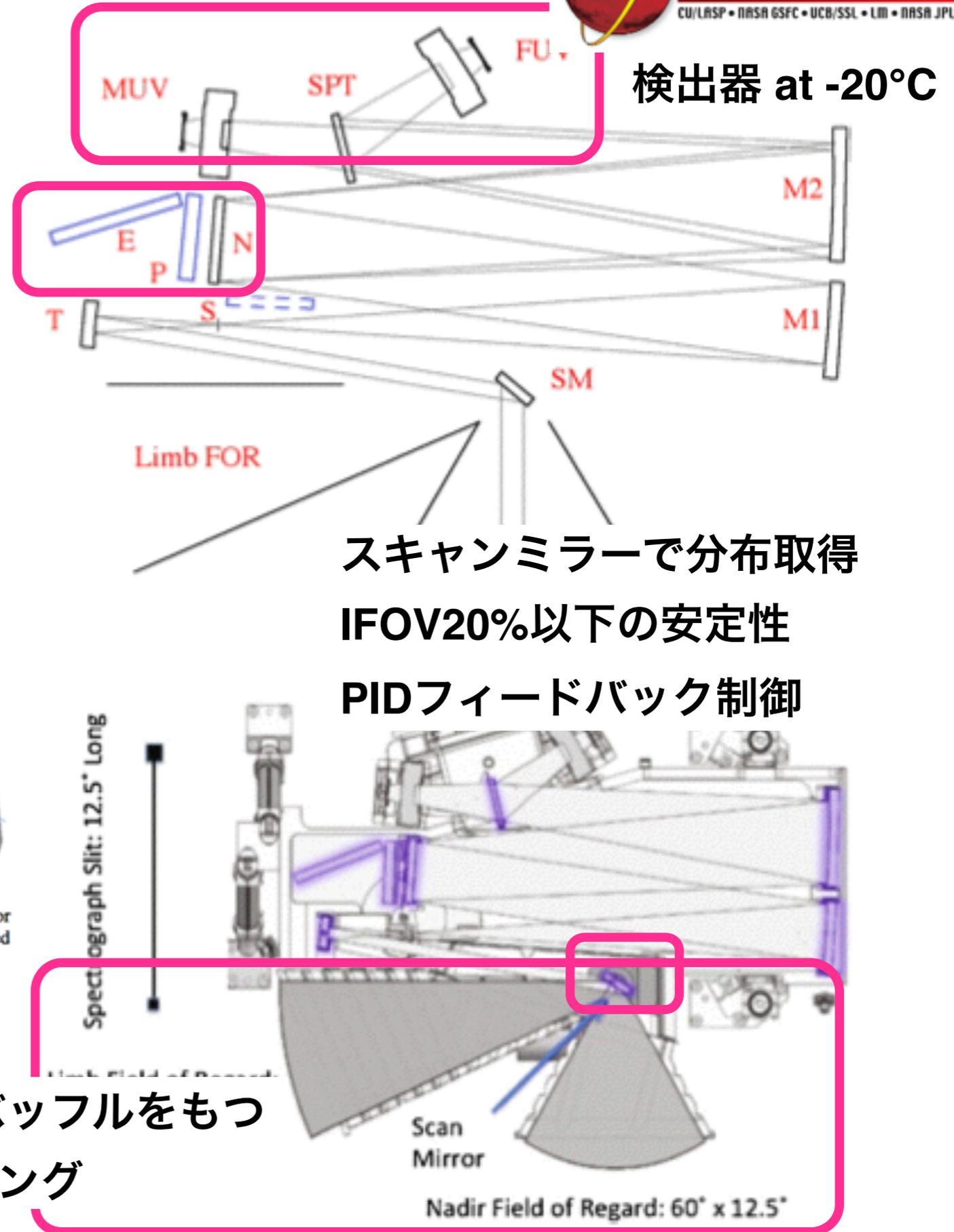


Fig. 21 The detector module includes a housing that supports a beam splitter, the FUV and MUV detector assemblies and a mercury stimulus lamp. A high voltage power supply, not visible in the figure, is attached to the bottom of the housing

narrow, long region
($0.06^\circ \times 11^\circ$) to measure
atmospheric emissions and two

Limb/Nadirそれぞれにバッフルをもつ
迷光を防ぐ特殊コーティング



スキャンミラーで分布取得
IFOV20%以下の安定性
PIDフィードバック制御

Predicted Performance

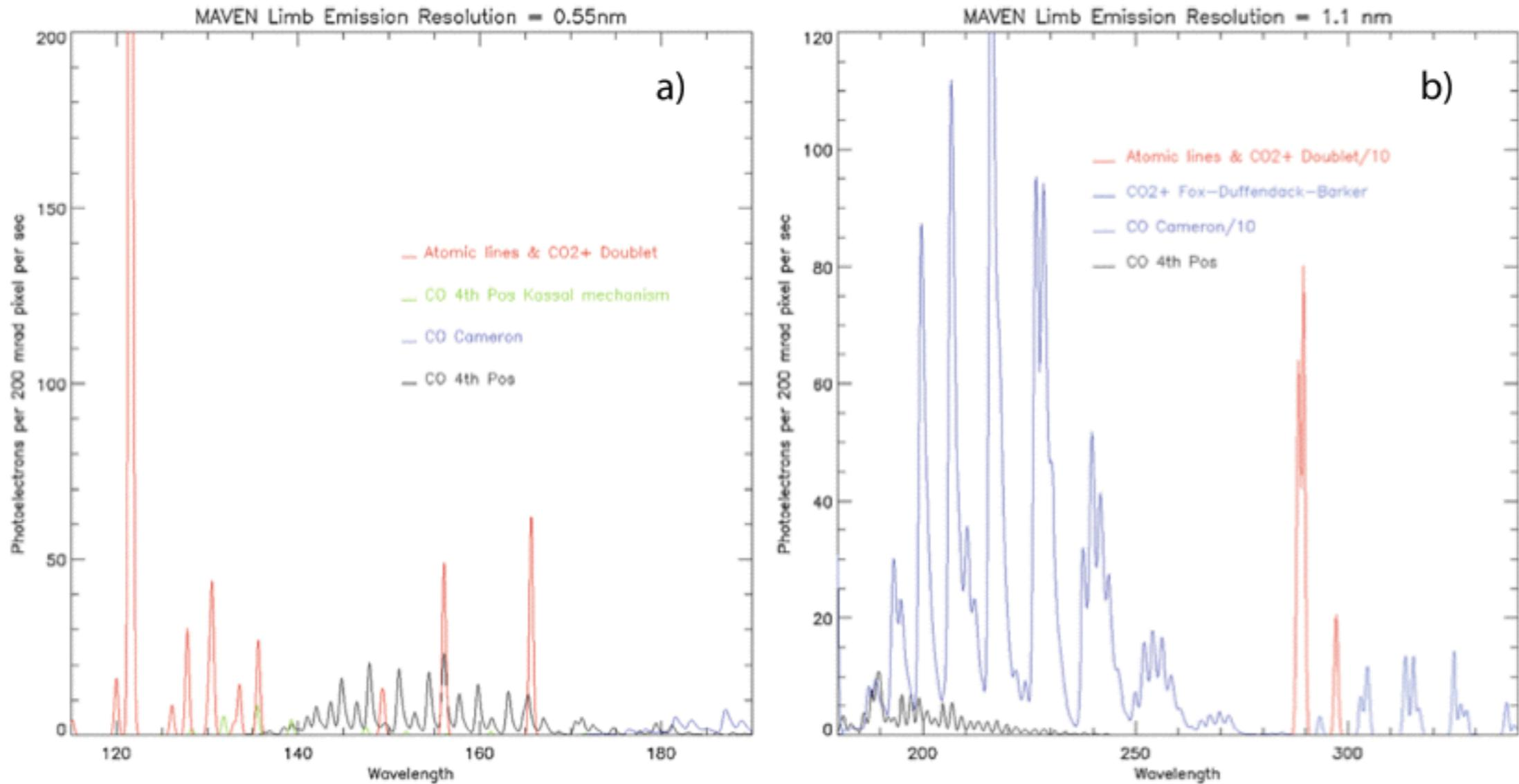
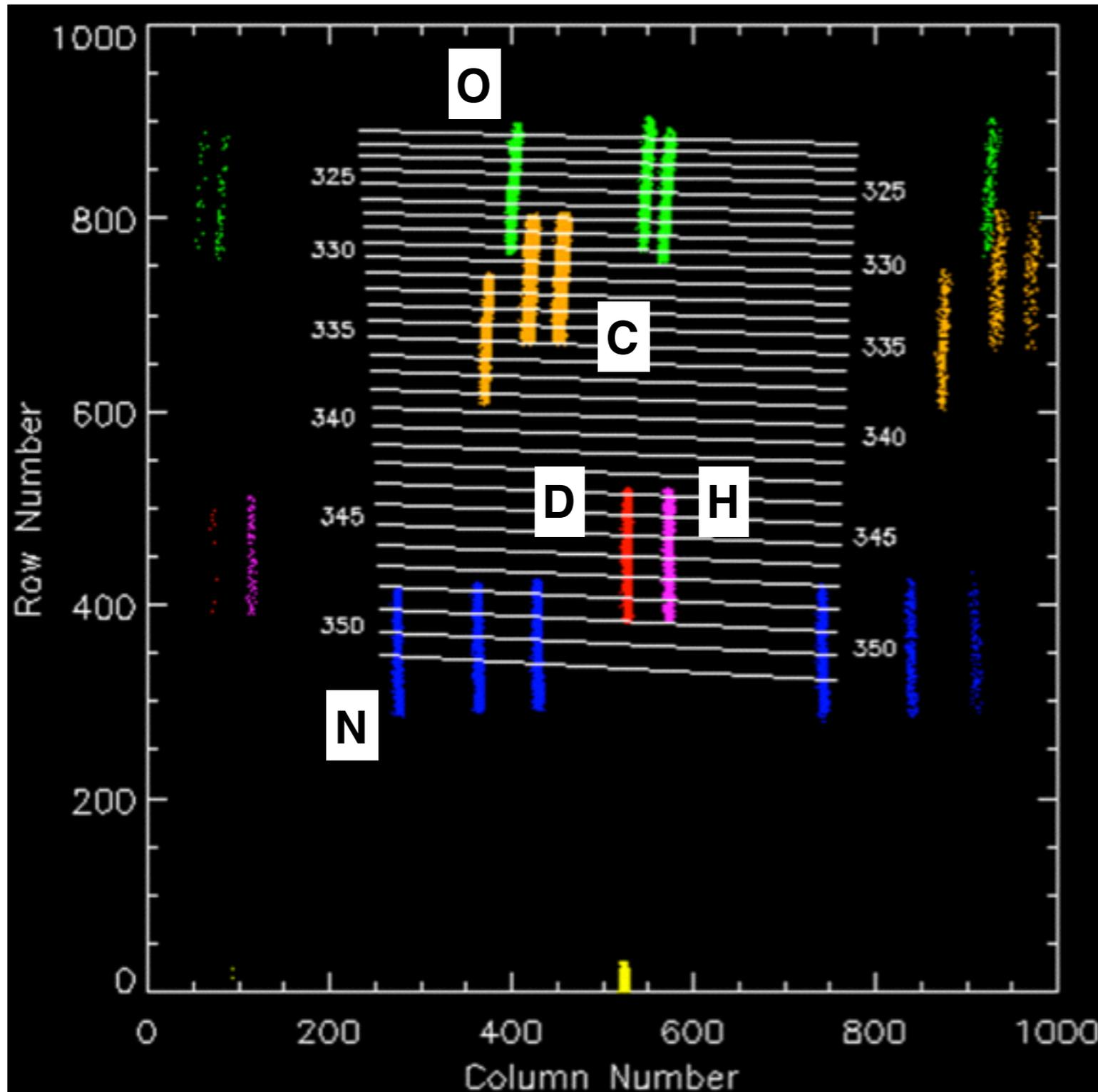


Fig. 14 Simulated normal-mode FUV (*left*) and MUV (*right*) spectra of the Mars airglow as observed during a periapsis limb observation. Emission lines from the major atomic species (H, O, C and N) and from the CO₂⁺ are shown in *red*. *Black* and *blue* lines show the 4th positive and Cameron band systems of CO, respectively, as well as the Fox-Duffenback-Barker system of CO₂⁺. The observed spectrum is the sum of the atomic and molecular components

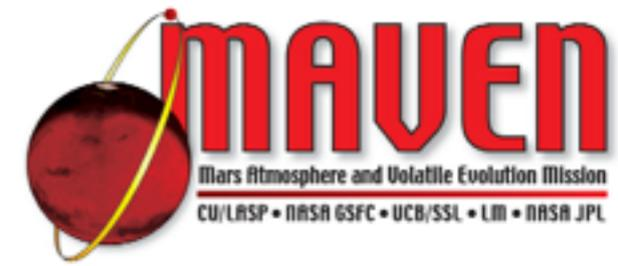
SPICAMに比べてとても高い感度を達成.

échelle image



Ly-D emission (121.533nm)で効率最大化を測るように設計.

Detection



gain: $10^4 \sim 4 \times 10^4$ (output photon/incident photon)

Photocathode → MCP → fiber → CMOS → AD

quantum efficiency: 0.1 ~ 0.01
(UV photons to photoelectrons)

50% loss

0.04DN/electron

0.45 electrons/photon

$$SNR = \frac{DN_{Ph}}{\sqrt{G_{ADC} \cdot G_{Det} \cdot E \cdot DN_{Ph} + G_{ADC} \cdot DN_{Dark} + 2 \cdot G_{ADC} \cdot DN_{Read}^2 + 2 \cdot G_{ADC} \cdot DN_{ADC}^2}} \quad (9)$$

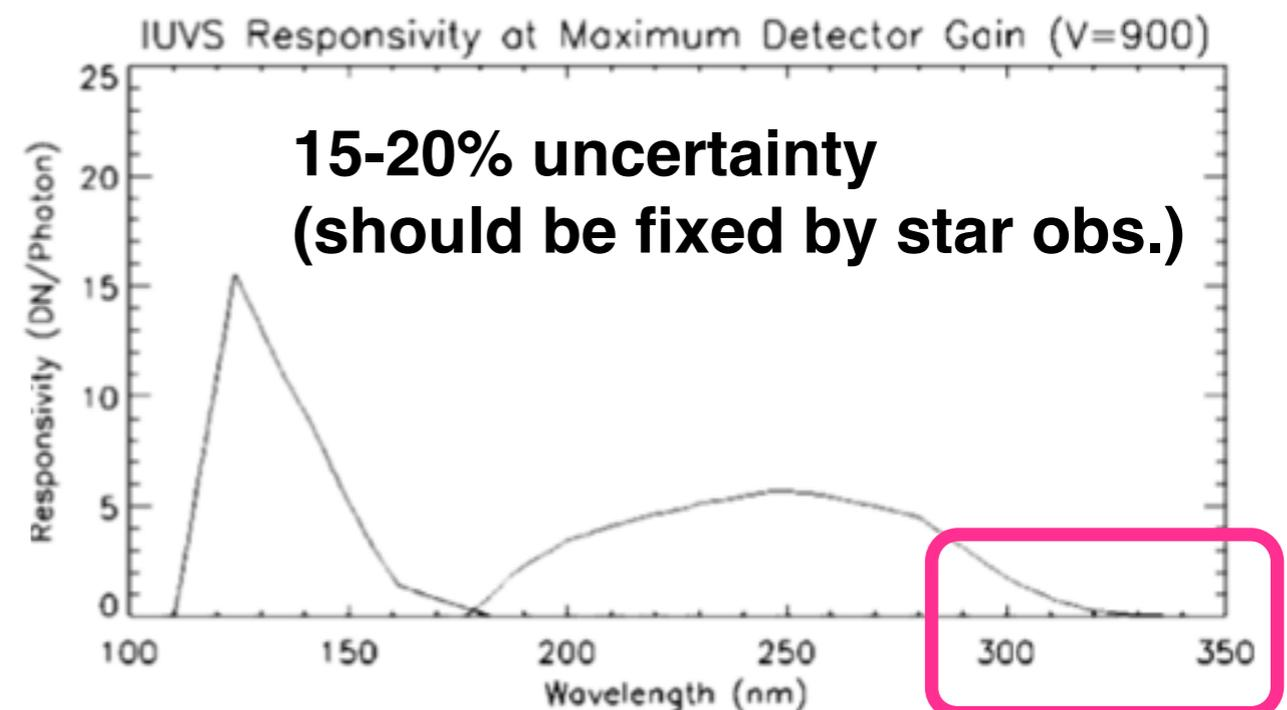
MCP high V (e.x. 700V):

$$R \sim [DN_{Ph} / G_{ADC} \cdot G_{Det} \cdot E]^{1/2} = [\dot{N} \cdot Qe_{Pc} \cdot \Delta t_{int} / E]^{1/2}$$

As for Echelle Mode

#TotalDN(Echelle)/TotalDN(Normal) = 0.096

#The etendue and optical throughput are 6.6 and 10 times less than normal mode.



Spectroscopy



incident/diffraction angles

grating space

FWHM

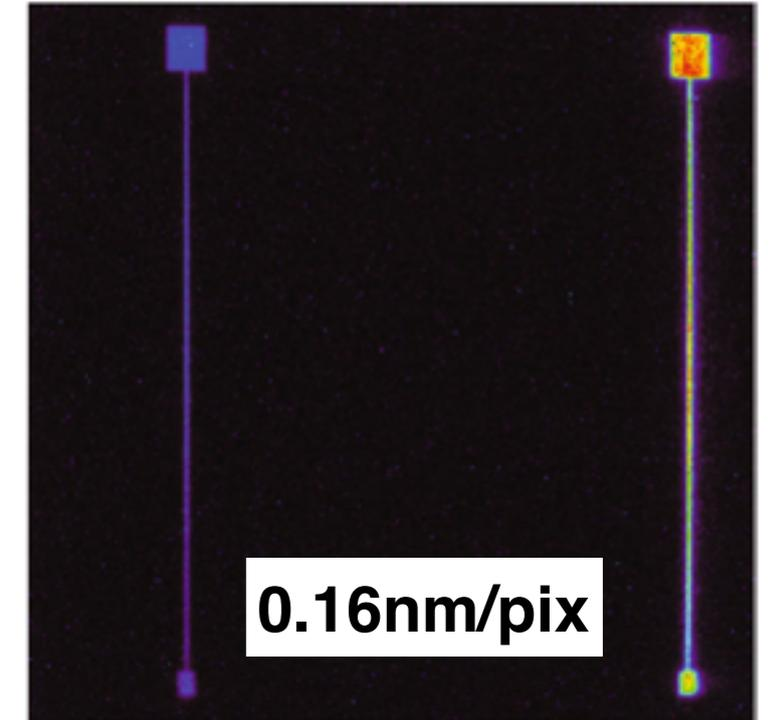
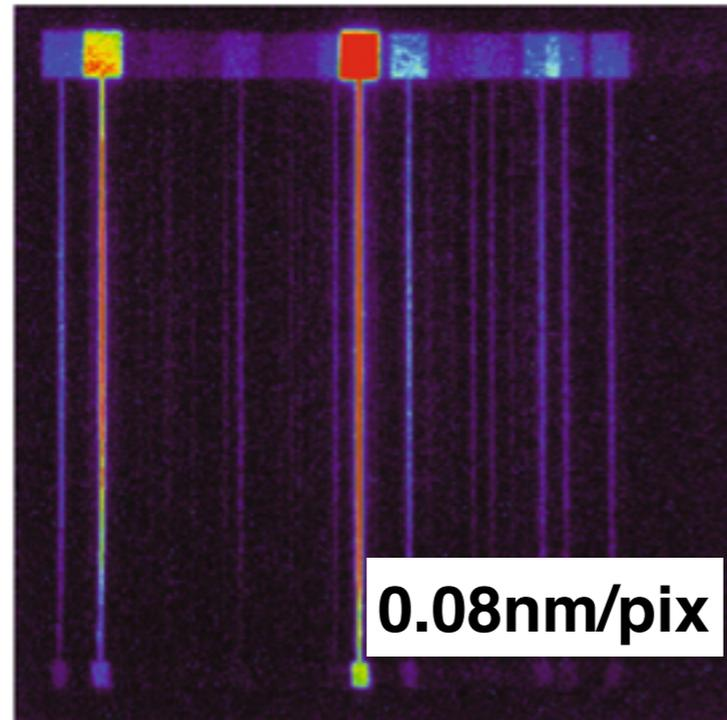
$$\Delta\lambda = \frac{d \cdot \cos(\beta) \cdot \cos(\gamma)}{n} \cdot \Delta\beta = \frac{d \cdot \cos(\beta) \cdot \cos(\gamma)}{n} \cdot \frac{\Delta w}{f}, \quad (4)$$

resolution

order number

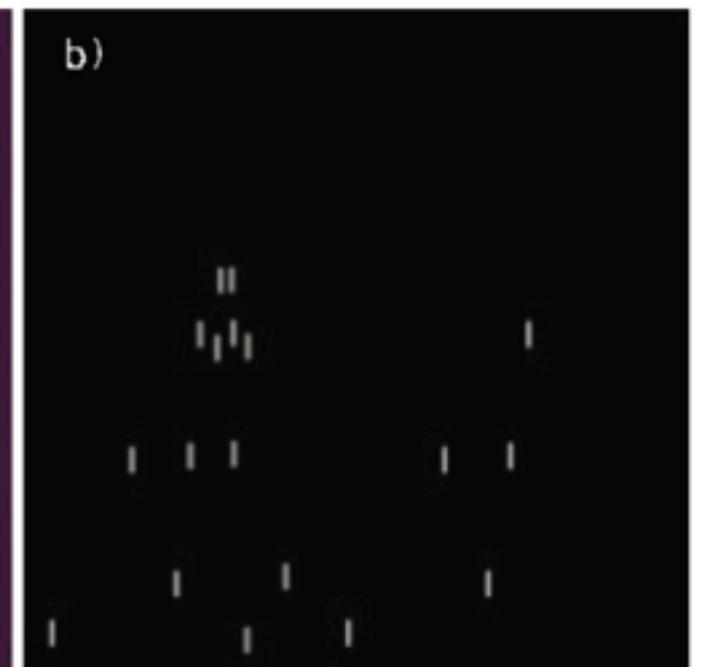
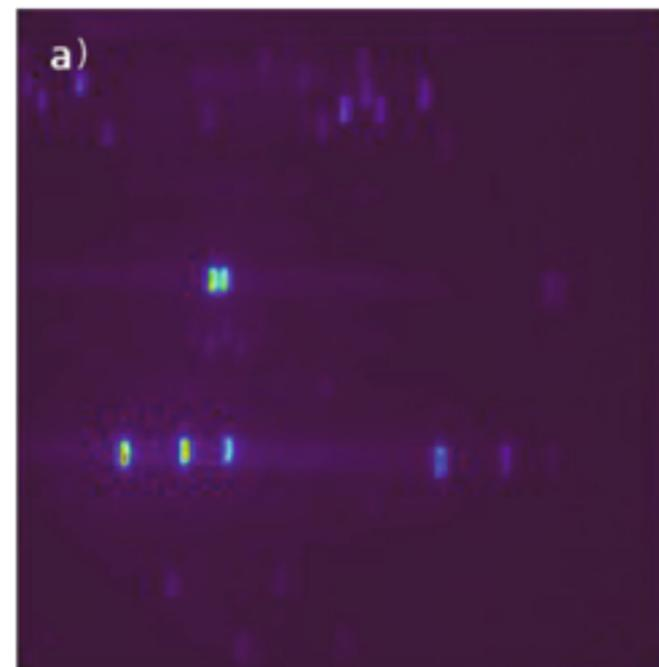
focal length

0.1mmx20mm slit



0.0309nm at $n=346$, $\beta=76.25^\circ$
 $\Delta\omega=13$ pixels= 0.305 mm or $R=12,900$

0.1mmx3mm slit



Point Spread Function



50% larger than expected
but still resolve D/H

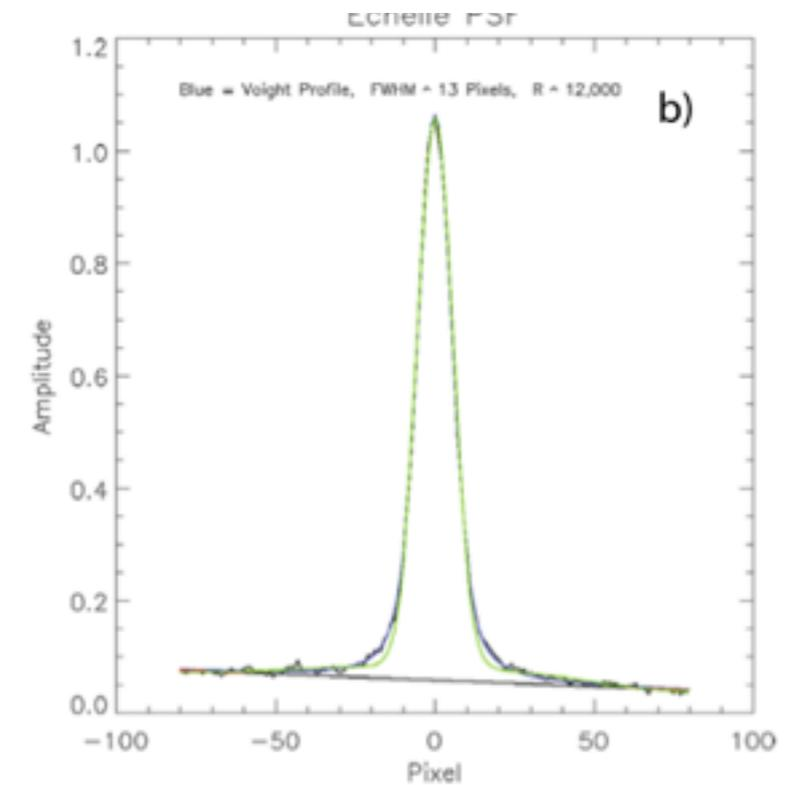
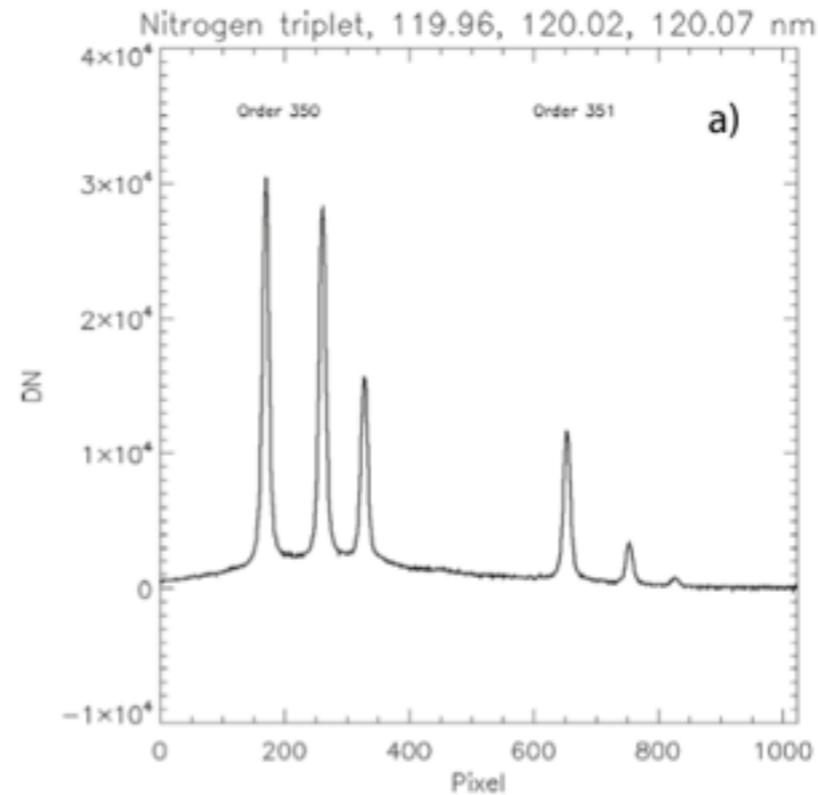
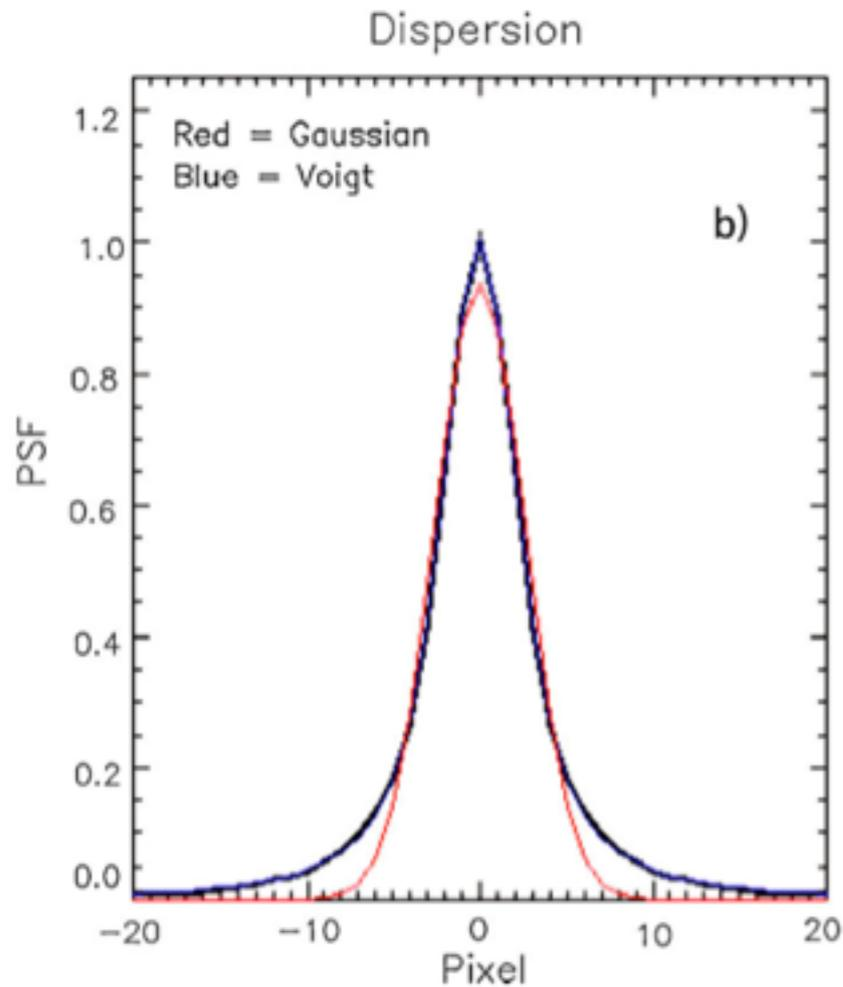


Fig. 28 The *left panel* is a line plot of orders 350 and 351 produced by summing rows 300–400 of the image in the left panel of Fig. 25. The *right plot* shows Gaussian (green) and Voigt (blue) fits to the profile centered near pixel 650

光学系システム全体のパフォーマンスを知る。

これで波長分解能(0.6nm in FUV and 1.2nm in MUV, 0.006nm with echelle)・空間分解能が決まる。

End

